ChemComm

COMMUNICATION

View Article Online
View Journal

Cite this: DOI: 10.1039/c9cc04705k

Received 19th June 2019,
Accepted 1st July 2019

DOI: 10.1039/c9cc04705k

rsc.li/chemcomm

Online desalting and sequential formation of analyte ions for mass spectrometry characterization of untreated biological samples†

Md. Matiur Rahman, * Konstantin Chingin and Huanwen Chen*

The metal salts ubiquitously present in biological samples cause serious ion suppression, capillary clogging and signal fluctuation in ESI/nESI. Herein, a current-limited high voltage polarity reversing approach was applied for the online separation of intrinsic metal ions in biological samples, resulting in the generation of protonated analytes at the nESI tip for mass analysis without interference from salt cations. Stable and durable signals (~30–60 s) were observed for protonated proteins, peptides and metabolites in complex biological samples, including liquids, solids and viscous samples, even with very high salt concentration (100 mM NaCl), allowing comprehensive tandem MS analysis with on average *ca.* 5-times higher analyte signal intensities compared to the conventional nESI analysis. Therefore this approach offers improved performance of nESI/ESI for the sensitive molecular analysis of untreated biological samples, opening new possibilities in various disciplines, including biology, medicine, chemistry, life sciences, *etc.*

Rapid chemical analysis of untreated biological samples is important in multiple fields of chemistry, life sciences, medicine and industrial biotechnology. Complex biological samples contain high amounts of matrix components and salts, which commonly suppress analyte signal detection. Therefore, direct chemical analysis of untreated biological samples presents a considerable challenge. Many analytical techniques have been used for the removal of salts and analyte detection from complex biological samples, such as three layer sandwich gel electrophoresis,[1] gel cartridge based inline chromatography,[2] microdialysis,[3] silver nanoparticle based microextraction,[4] capillary electrophoresis,[5–7] solid phase micro extraction,[8,9] infrared spectroscopy (IR),[10] gas chromatography mass spectrometry (GC-MS),[11,12] high performance liquid chromatography (HPLC)[13–15] and liquid chromatography mass spectrometry (LC-MS).[16,17] These methods feature high chemical sensitivity, but they typically require laborious sample preparation (crushing, grinding, extraction and separation *etc.*) and sophisticated multi analyzers with tandem operation. Recently, great efforts have been devoted to achieve desalting and direct analysis of untreated biological samples without chromatographic separation. Several approaches have been proposed[18–35] each having its own advantages and disadvantages. Common advantages of these approaches include the high speed of analysis, high throughput and minimization of sample preparation. Common disadvantages are mainly related to the ion suppression effects due to the lack of chromatographic separation and hence the narrow molecular range of detection with compromised chemical sensitivity.

Here we demonstrate a simple online desalting and sequential molecular analysis of untreated bulk biological samples including, fruits and viscous samples using polarity-reversing nanoelectrospray ionization combined with ion current limitation by a 10 GΩ in-series resistor (PR-R-nESI). For the detection of positive ions by PR-R-nESI, a high negative voltage (−8 kV) is first applied for ~20 s to the silver-coated Pt wire electrode inserted inside the nESI capillary (Fig. 1). During the negative pulse, the salt cations are driven to move toward the negatively charged electrode, and the negatively charged spray is generated at the nESI tip. After that, a positive high voltage (+1.7 kV) is applied to the emitter, resulting in the generation of protonated analytes at the nESI tip for mass analysis without interference from salt cations for ~30 s–1 min, thus allowing comprehensive analyte characterization by tandem mass spectrometry. Advantageous to the conventional nESI, PR-R-nESI obviates tip clogging and electric discharge during the analysis of untreated samples. Other advantages of current-limited polarity reversing nESI-MS include the high chemical sensitivity (*ca.* 5 times higher compared to the conventional nESI), simplicity, ease of use and high speed of sample analysis. Overall, our results indicate that PR-R-nESI can be considered a versatile approach for the direct sensitive detection of proteins, peptides, metabolites and small molecules in complex biological samples, including liquids, solids and viscous samples, even at salt concentrations up to 100 mM, without any sample pre-treatment and additives. Based on our experience with PR-R-nESI, we believe that this approach could significantly advance biological or biomedical mass spectrometry in the near future.

Jiangxi Key Laboratory for Mass Spectrometry and Instrumentation, East China University of Technology, Nanchang 330013, China. E-mail: matiurrahmanbot@yahoo.com, matiurrahman@ecit.cn, chw8868@gmail.com

† Electronic supplementary information (ESI) available. See DOI: 10.1039/c9cc04705k

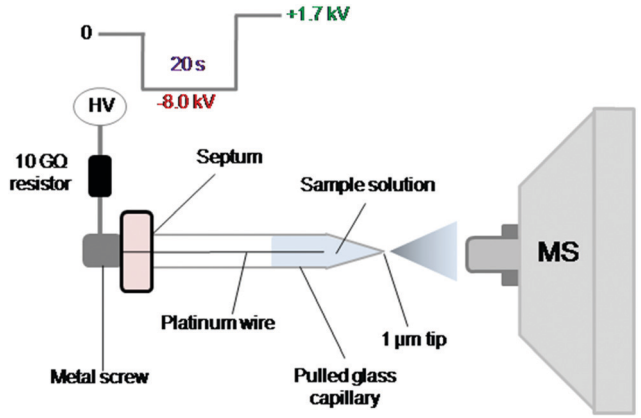

Fig. 1 Schematic diagram of PR-R-nESI ion source.

Biological samples commonly contain high concentration of salts or other complex components interfering with analyte ion detection. The obviation of matrix effects is difficult to achieve by direct-infusion ESI or nESI. The desalting of analyte solutions is routinely achieved by approaches based on chromatographic separation.[2] However, the important advantage of PR-R-nESI is its simplicity and higher speed of analysis. Fig. 2 summarizes the results of PR-R-nESI analysis of 10 mM NaCl solutions of cytochrome *c* and insulin. A clear desalting effect is seen for both analytes. The signal of the NaCl cluster becomes dominant only after several minutes of analysis in PR-R-nESI (Fig. 2a–c and e–g). This result indicates that the electrophoretic desalting takes place inside the nanocapillary over the negative voltage pulse. Most probably, solute cations such as Na^+ and K^+, owing to their high electrophoretic mobility, migrate toward the tip of the nanocapillary when the high negative voltage is applied (Fig. S2, ESI†). Thus, it can be seen that in conventional nESI and ESI the NaCl cluster ions totally suppress the cytochrome *c* and insulin ions (Fig. 2d, h and Fig. S3a, b, ESI†) due to the application of positive high voltage. In contrast, in PR-R-nESI the cytochrome *c* and insulin can be clearly observed over several minutes. Indeed, protein–metal adducts are not completely removed in PR-R-nESI at high salt concentrations (Fig. S4, ESI†). However, the sodium ion adduction does not notably hinder the observation of protein monomers up to the NaCl concentration of *ca.* 10 mM. In contrast, the protein signal is almost entirely suppressed in conventional nESI under the same conditions (Fig. S4, ESI†). The analyte signal intensity is *ca.* 5 times higher than that of conventional nESI or ESI. These data suggest that it takes on the order of several minutes for metal cations to migrate toward the capillary tip when the positive voltage is applied to the capillary. Interestingly, cytochrome *c* with 10 mM NaCl shows very high charge states using PR-R-nESI (up to 19+) (Fig. 2b). Similar observations have been recently reported by Gong *et al.*[36]

In another experiment, cyctochrome *c* solution with even higher concentration of NaCl is used (100 mM) to illustrate the difference in performance between conventional nESI and PR-R-nESI. Also, different magnitude of negative voltage was tested for the analysis by PR-R-nESI (Fig. 3 and Fig. S5, ESI†). The mixture is loaded into the nanocapillary by a gel loading tip. It can be seen that in conventional nESI the NaCl cluster ions totally suppress the cytochrome *c* ions

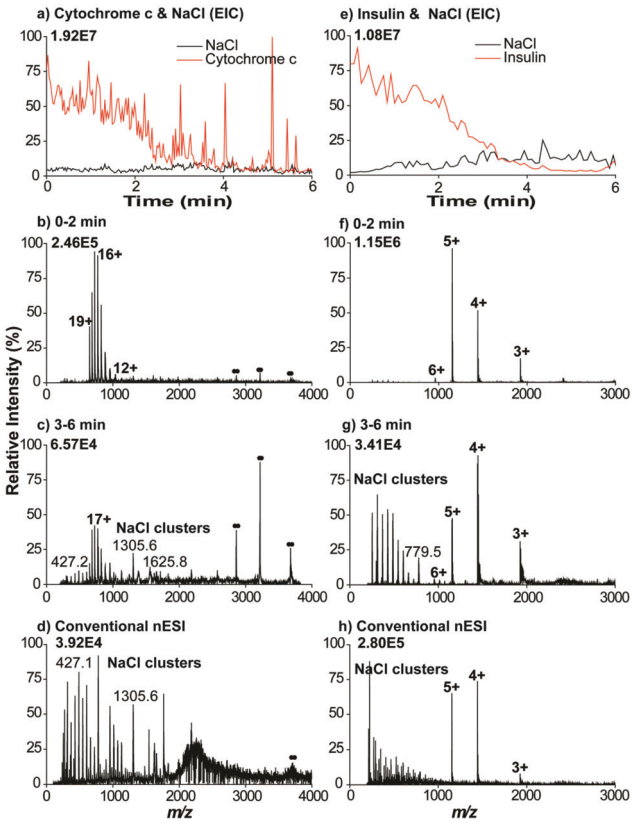

Fig. 2 The comparison of PR-R-nESI-MS analysis *vs.* conventional nESI-MS for different analytes: (a) extracted ion chromatogram and (b and c) mass spectra of cytochrome *c* (120 μg mL^{-1}) by PR-R-nESI; (d) the mass spectrum of cytochrome *c* by conventional nESI; (e) extracted ion chromatogram and (f and g) mass spectra of insulin (58 μg mL^{-1}) by PR-R-nESI; (h) the mass spectrum of insulin by conventional nESI; two black circles indicate the dimer of cytochrome *c*.

(Fig. 3e). In contrast, in PR-R-nESI the cytochrome *c* can be observed over several minutes. The signal duration of cytochrome *c* is increased with the magnitude of negative high voltage (−8 kV) (Fig. 3d). This observation can be explained by stronger electrophoretic separation within the capillary between sodium cations and protein species at higher negative voltage. We believe that the high voltage gradient in the capillary during the negative pulse may also result in the propagation of liquid closer toward the tip of the capillary, thus eliminating residual air bubbles. Air bubbles present in the nanocapillary are ubiquitous in nESI and are commonly attributed to the source malfunction and instability (either because of the Jamin effect[37] or due to the electrical resistance of bubbles). It is very difficult to fully get rid of bubbles in nESI because the electrostatic forces are typically not sufficient to clear the line. Note that the use of high negative voltage (*e.g.*, −8 kV) only becomes possible with the use of a high-ohmic resistor. Without the current limitation, the use of high negative voltage (*ca.* <-3.5 kV) is usually impossible in nESI due to the current overflow.

Fig. S6 (ESI†) shows sequential PR-R-nESI for the equimolar mixture of cytochrome *c* and 1,2-dipalmitoyl-*sn*-glycerophosphocholine in 5% methanolic aqueous solution. Our data indicate that 1,2-dipalmitoyl-*sn*-glycerophosphocholine is detected

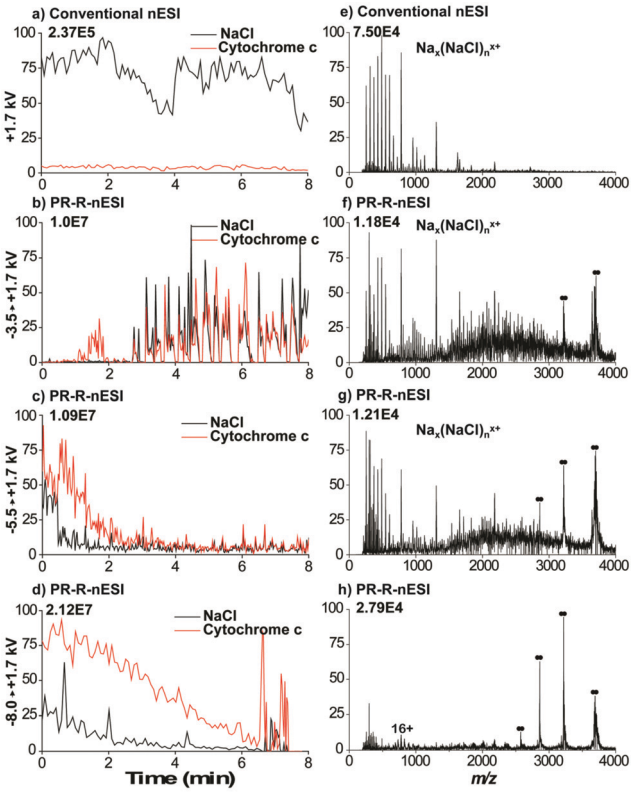

Fig. 3 Conventional nESI and PR-R-nESI-MS for the sequential analysis of cytochrome *c* (120 μg mL^{-1}), with 100 mM NaCl. (a and e) EIC and mass spectra of conventional nESI. (b–d) and (f–h) EIC and mass spectra of cytochrome *c* with 100 mM NaCl obtained by PR-R-nESI. Two black circles indicate the dimer of cytochrome *c*.

(from 0.1–0.4 min) while cytochrome *c* is detected after 0.4 min (Fig. S6, ESI†). Mandal *et al.* also reported that proteins and lipids in a mixture can be detected separately using probe electrospray ionization (PESI) due to the difference in surface activity.[38] In contrast to PESI, in PR-R-nESI we attribute the sequential ionization of proteins and lipids to be due to the difference in their electrophoretic mobility.

Quantitative analysis was performed for a peptide (MRFA) in water by PR-R-nESI. The results are shown in Fig. S7a (ESI†). Working MRFA solutions were prepared at concentrations of 500 ng mL^{-1}, 250 ng mL^{-1}, 100 ng mL^{-1}, 50 ng mL^{-1}, 25 ng mL^{-1}, 10 ng mL^{-1} and 1 ng mL^{-1} respectively. All experiments were run from the lowest to highest concentration to avoid cross contamination of the ion transport tube. Reproducible PR-R-nESI-MS signals as well as very good linearity of the signal intensity ($R > 0.992$) were observed within the concentration range of 10–500 ng mL^{-1}. The limit of detection for MRFA was 10 ng mL^{-1}. The inset MS/MS spectrum in Fig. S7a (ESI†) shows the confirmation of MRFA detection at 10 ng mL^{-1}. Similar analysis was carried out for MRFA in 10 mM NaCl. The detection limit of MRFA was *ca.* 10 times higher in 10 mM aqueous NaCl compared to MRFA in pure water (Fig. S7, ESI†). The linearity of the MRFA signal response in 10 mM NaCl was $R > 0.965$ in the concentration range 100–10 000 ng mL^{-1}. The linearity of the MRFA signal in 10 mM NaCl is decent albeit not as good as for MRFA in pure water.

Almost all ambient ionization methods require dissection, slicing or severe wounding of biological samples before analysis. In contrast, in PR-R-nESI, a solid needle is used for the direct sampling of biological tissues by stabbing without any notable invasiveness to the sample. The tip of the needle is then directly inserted into the nanocapillary preloaded with solvent for PR-R-nESI analysis. This sampling method is useful for the sampling of highly-complex samples, viscous samples and living objects. Only a tiny amount of sample is required for the analysis. This method can be implemented as a point of care analysis in GP clinics, pathological centers and operating rooms. Note that polarity reversing and ion current limitation are critical for the stable and sensitive nESI detection, as described in our previous publication.[39] Conventional ESI or nESI emitters are prone to rapid clogging and/or discharge during the analysis of complex matrix samples. Fig. 4 demonstrates sequential PR-R-nESI ionization of molecules in untreated strawberry and compares the results with direct nESI analysis under the same experimental conditions. A tiny amount of the juicy part of strawberry tissue is sampled by silver-coated platinum wire. The tip of the wire is then inserted into the nanocapillary prefilled with 1 μL aqueous solution. In conventional nESI the spectrum of strawberry is dominated by metal ion adducts (*m*/*z* 218, 381, 433, 722, 914, 1064) (Fig. 4d–f). In contrast, PR-R-nESI shows molecular separation of protonated and metal adduct species. Abundant protonated peaks (*m*/*z* 133, 147) show up during the initial 0–0.5 min, followed by metal adduct ions from 0.5 to 2 min (*m*/*z* 218, 381, 433, 722, 914, 1064) (Fig. 4a–c). These results indicate that PR-R-nESI is a promising method for desalting of untreated strawberry samples. Owing to the desalting effect, PR-R-nESI shows higher signal sensitivity compared to conventional nESI.

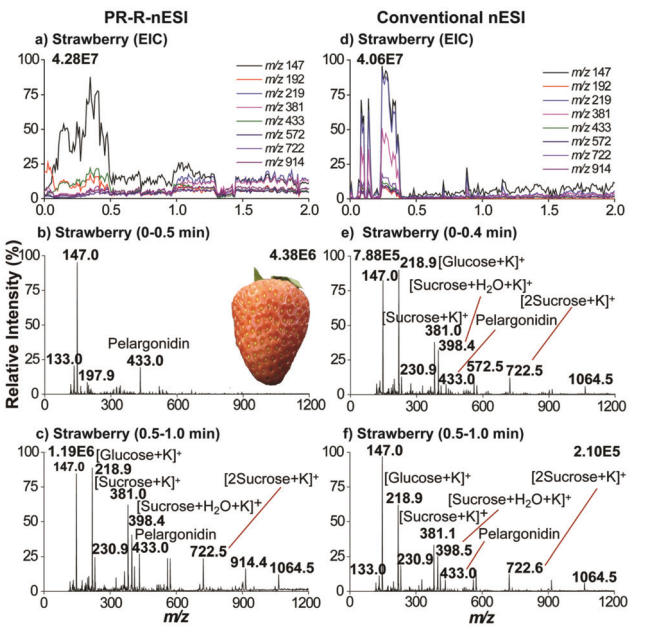

Fig. 4 Direct PR-R-nESI and conventional nESI for sequential analysis of an untreated strawberry sample: (a) EIC for PR-R-nESI, (b) 0–0.5 min and (c) 0.5–1 min, (d) EIC for conventional nESI, (e) 0–0.4 min and (f) 0.5–1 min.

The separation of protonated signals from ion adducts in PR-R-nESI is particularly useful for tandem mass spectrometry analysis. In another experiment, a tiny amount of sample of potato tissue is sampled by stabbing a silver-coated platinum wire against the potato. The tip of the wire is then inserted into the nanocapillary prefilled with 1 μL aqueous solution. The PR-R-nESI was run immediately after inserting the needle. Protonated phytochemicals solanine and chaconine are observed at high abundance. The tandem MS experiment confirms the molecular identity for solanine and chaconine in potato tissue (Fig. S8, ESI†). The data for the PR-R-nESI analysis of different biological samples is shown and discussed in ESI.†

Nanoelectrospray analysis assisted by high-voltage polarity reversing in combination with ion current limitation by a high-ohmic resistor (PR-R-nESI) was demonstrated for the comprehensive sequential molecular analysis of complex chemical matrices and untreated bulk biological samples. A variety of compounds, including lipid, protein, alkaloids, flavonoids and anthocyanins were detected in protonated form without salt interference simply by sampling a tiny amount of sample into the nanocapillary prefilled with ionizing solution at ambient pressure and without any sample preparation. The PR-R-nESI approach also allows considerable sensitivity enhancement and signal durability from the complex matrix sample compared to conventional nESI. Indeed more research is necessary for the further increase of the separation time as well as for even higher chemical sensitivity of analysis. This should be possible by applying higher negative voltage to the nanocapillary. Currently we are limited by the restriction of the LTQ instrument (−8 kV). Also, the inner diameter of a pulled glass capillary could be reduced[40–43] down to 1–100 nm, which may also benefit the degree of electrophoretic separation of metal ions in PR-R-nESI. The relevant experiments will be carried out in our lab in the near future.

This work was supported by the National Natural Science Foundation of China (no. 21520102007 and 21727812), Program for Changjiang Scholars and Innovative Research Team in University (PCSIRT) (no. IRT_17R20), 111 Project (no. D17006), and the Project of Jiangxi Provincial Department of Education (no. GJJ160544).

Conflicts of interest

There are no conflicts to declare.

References

1 T. Liu, A. M. Martin, A. P. Sinai and B. C. Lynn, *J. Proteome Res.*, 2008, **7**, 4256–4265.
2 J. Cavanagh, L. M. Benson, R. Thompson and S. Naylor, *Anal. Chem.*, 2003, **75**, 3281–3286.
3 C. Liu, S. A. Hofstadler, J. A. Bresson, H. R. Udseth, T. Tsukuda, R. D. Smith and A. P. Snyder, *Anal. Chem.*, 1998, **70**, 1797–1801.
4 K. Shrivas and H.-F. Wu, *Anal. Chem.*, 2008, **80**, 2583–2589.
5 D. T. Chiu, S. J. Lillard, R. H. Scheller, R. N. Zare, S. E. Rodriguez-Cruz, E. R. Williams, O. Orwar, M. Sandberg and J. A. Lundqvist, *Science*, 1998, **279**, 1190–1193.
6 I. Oita, H. Halewyck, S. Pieters, B. Thys, Y. V. Heyden and B. Rombaut, *J. Virol. Methods*, 2012, **185**, 7–17.
7 T. Lapainis, S. S. Rubakhin and J. V. Sweedler, *Anal. Chem.*, 2009, **81**, 5858–5864.
8 A. P. Dahlin, S. K. Bergström, P. E. Andrén, K. E. Markides and J. Bergquist, *Anal. Chem.*, 2005, **77**, 5356–5363.
9 G. Morales-Cid, I. Gebefugi, B. Kanawati, M. Harir, N. Hertkorn, R. Rosselló-Mora and P. Schmitt-Kopplin, *Anal. Bioanal. Chem.*, 2009, **395**, 797–807.
10 H. Kelebek and S. Selli, *J. Sci. Food Agric.*, 2011, **91**, 1855–1862.
11 M. Cerdán-Calero, L. Izquierdo, J. M. Halket and E. Sentandreu, *Int. J. Food Sci. Technol.*, 2014, **49**, 1432–1440.
12 J. L. Gómez-Ariza, T. García-Barrera and F. Lorenzo, *J. Chromatogr. A*, 2004, **1047**, 313–317.
13 J. L. Gómez-Ariza, M. J. Villegas-Portero and V. Bernal-Daza, *Anal. Chim. Acta*, 2005, **540**, 221–230.
14 R. Scherer, A. C. P. Rybka, C. A. Ballus, A. D. Meinhart, J. T. Filho and H. T. Godoy, *Food Chem.*, 2012, **135**, 150–154.
15 L. Camarda, V. Di Stefano, S. F. Del Bosco and D. Schillaci, *Fitoterapia*, 2007, **78**, 426–429.
16 L. Hu, S. Lei and L. Guo, *Sepu*, 2012, **30**, 832–835.
17 R. Shakya and D. A. Navarre, *J. Agric. Food Chem.*, 2008, **56**, 6949–6958.
18 D.-Y. Chang, C.-C. Lee and J. Shiea, *Anal. Chem.*, 2002, **74**, 2465–2469.
19 M. Kanti Mandal, L. Chuin Chen, Y. Hashimoto, Z. Yu and K. Hiraoka, *Anal. Methods*, 2010, **2**, 1905–1912.
20 D. J. Clarke and D. J. Campopiano, *Analyst*, 2015, **140**, 2679–2686.
21 R. Javanshad, E. Honarvar and A. R. Venter, *J. Am. Soc. Mass Spectrom*, 2019, **30**(4), 694–703.
22 S. Karki, F. Shi, J. J. Archer, H. Sistani and R. J. Levis, *J. Am. Soc. Mass Spectrom*, 2018, **29**, 1002–1011.
23 Z. Zhang, C. J. Pulliam, T. Flick and R. G. Cooks, *Anal. Chem.*, 2018, **90**, 3856–3862.
24 T. G. Flick, C. A. Cassou, T. M. Chang and E. R. Williams, *Anal. Chem.*, 2012, **84**, 7511–7517.
25 R. L. Griffiths, A. Dexter, A. J. Creese and H. J. Cooper, *Analyst*, 2015, **140**, 6879–6885.
26 S. Ambrose, N. G. Housden, K. Gupta, J. Fan, P. White, H.-Y. Yen, J. Marcoux, C. Kleanthous, J. T. S. Hopper and C. V. Robinson, *Angew. Chem., Int. Ed.*, 2017, **56**, 14463–14468.
27 L. S. Eberlin, D. R. Ifa, C. Wu and R. G. Cooks, *Angew. Chem., Int. Ed.*, 2010, **49**, 873–876.
28 J. Balog, S. Kumar, J. Alexander, O. Golf, J. Huang, T. Wiggins, N. Abbassi-Ghadi, A. Enyedi, S. Kacska, J. Kinross, G. B. Hanna, J. K. Nicholson and Z. Takats, *Angew. Chem., Int. Ed.*, 2015, **54**, 11059–11062.
29 H. Zhang, L. Zhu, L. Luo, N. Wang, K. Chingin, X. Guo and H. Chen, *J. Agric. Food Chem.*, 2013, **61**, 10691–10698.
30 G. A. Gómez-Ríos and J. Pawliszyn, *Angew. Chem., Int. Ed.*, 2014, **53**, 14503–14507.
31 H. Zhang, H. Gu, F. Yan, N. Wang, Y. Wei, J. Xu and H. Chen, *Sci. Rep.*, 2013, **3**, 2495.
32 G. Huang, G. Li and R. G. Cooks, *Angew. Chem., Int. Ed.*, 2011, **50**, 9907–9910.
33 Y. Ren, M. N. McLuckey, J. Liu and Z. Ouyang, *Angew. Chem., Int. Ed.*, 2014, **53**, 14124–14127.
34 W. Zhang, S. Chiang, Z. Li, Q. Chen, Y. Xia and Z. Ouyang, *Angew. Chem., Int. Ed.*, 2019, **58**(18), 6064–6069.
35 Z. Wei, S. Han, X. Gong, Y. Zhao, C. Yang, S. Zhang and X. Zhang, *Angew. Chem., Int. Ed.*, 2013, **52**, 11025–11028.
36 X. Gong, C. Li, R. Zhai, J. Xie, Y. Jiang and X. Fang, *Anal. Chem.*, 2019, **91**(3), 1826–1837.
37 W. O. Smith and M. D. Crane, *J. Am. Chem. Soc.*, 1930, **52**, 1345–1349.
38 M. K. Mandal, L. C. Chen and K. Hiraoka, *J. Am. Soc. Mass Spectrom.*, 2011, **22**, 1493–1500.
39 M. M. Rahman and K. Chingin, *Anal. Methods*, 2019, **11**, 205–212.
40 J. Hu, Q.-Y. Guan, J. Wang, X.-X. Jiang, Z.-Q. Wu, X.-H. Xia, J.-J. Xu and H.-Y. Chen, *Anal. Chem.*, 2017, **89**, 1838–1845.
41 A. C. Susa, Z. Xia and E. R. Williams, *Angew. Chem.*, 2017, **129**, 8020–8023.
42 A. C. Susa, J. L. Lippens, Z. Xia, J. A. Loo, I. D. G. Campuzano and E. R. Williams, *J. Am. Soc. Mass Spectrom.*, 2018, **29**, 203–206.
43 E. M. Yuill, N. Sa, S. J. Ray, G. M. Hieftje and L. A. Baker, *Anal. Chem.*, 2013, **85**, 8498–8502.

